Automatic Prostate Segmentation in Ultrasound Images using Gradient Vector Flow Active Contour

Bahram Dehghan[1], Ahad Salimi[2]
1- Department of Electrical Engineering, Sarvestan Branch, Islamic Azad University, Sarvestan, Iran
Email: Bahramdehghan1@gmail.com
2- Department of Electrical Engineering, Zarin dasht Branch, Islamic Azad University, Zarin dasht, Iran
Email: Ahad.salimi60@gmail.com

Received March 2013 Revised June 2013 Accepted Sep. 2013

ABSTRACT:
Prostate cancer is one of the leading causes of death by cancer among men in the world. Ultrasonography is said to be the safest technique in medical imaging so it is used extensively in prostate cancer detection. On the other hand**,** determining of prostate's boundary in TRUS (Transrectal Ultrasound) images is very necessary in lots of treatment methods prostate cancer. So the first and essential step for computer aided diagnosis (CAD) is the automatic prostate segmentation that is an open problem yet. But the low SNR, presence of strong speckle noise, Weak edges and shadow artifacts in these kinds of images limit the effectiveness of classical segmentation schemes. The classical segmentation methods fail completely or require post processing step to remove invalid object boundaries in the segmentation results. This paper has proposed a fully automatic algorithm for prostate segmentation in TRUS images that overcomes the explained problems completely. The presented algorithm contains three main stages. First**,** morphological smoothing and stick's filter are used for noise removing. A neural network is employed in the second step to find a point in prostate region. Finally in the last step, the prostate boundaries are extracted by GVF active contour. Some experiments for the performance validity of the presented method, compared with the extracted prostate by the proposed algorithm with manually-delineated boundaries by radiologist. The results show that our method extracts prostate boundaries with mean square area error lower than 4.4%.

KEYWORDS: prostate segmentation-stick filter-neural network-active contour**.**

1. INTRODUCTION

Prostate cancer continues to be the most commonly diagnosed cancer in men in the world and is the second mortality factor of cancer, after lung cancer in this group [1], [2]. TRUS images in comparison with the other modalities such as CT and MRI are captured easier, in real-time, and with lower cost, so they are widely used for diagnosis of prostate cancer. Although prostate cancer is prevalent but it would be curable if it is recognized in the earlier step of disease. So recognition of the prostate region in TRUS images is necessary in many new treatment methods such as determination of prostate volume, determination of the biopsy needles location and etc. If there are many images, it will be time consuming when the prostate segmentation is done by the radiologist. So, in order to save time, using computer for automatic prostate segmentation is necessary when there are many images. However, in ultrasound images, the contrast is usually low and the edges are fuzzy, so missing or diffusing boundaries is a very challenging problem for accurate segmentation of the prostate from the background.

Nowadays, many methods have been presented to facilitate more accurate segmentation of the prostate boundaries in ultrasound images. Several methods are presented in [3]-[6] but, however, these methods need that the initial points are specified by an expert. An automatic algorithm based on kalman filter is presented here [7]. Although This method reaches to accurate results but it is time consuming for its checking points of prostate boundary. Other authors showed some other automatic and semiautomatic methods for prostate segmentation such as segmentation the region, segmentation the boundary and deformable models [8]-[15].

In [16] the authors have introduced a medical- texture's local binary- pattern operator designed for applications of medical imaging where different tissues or micro organisms might maintain extremely weak underlying textures that make it impossible or very difficult for ordinary texture analysis approaches to classify them.

In the proposed method, Finally the deformations of a level set contour are controlled based on the medical texture- local binary pattern operator and extracts the prostate boundaries.

The authors of reference [17] proposed Semiautomatic 3-D Prostate Segmentation from TRUS Images Using Spherical Harmonics where the segmentation is defined in an optimization framework as fitting the best surface to the underlying images under shape constraints. To derive these constraints, the shape of the prostate are modeled by using spherical harmonics of eight degrees and performed statistical analysis on the shape parameters. After user initialization, the algorithm identifies the prostate boundaries. Samar et a1. presented a method based on spectral clustering segmentation algorithm is built on a totally different foundation that doesn't involve any function design or optimization [18]. The proposed algorithm depends mainly on graph theory techniques. It also doesn't need any contour or any points on the boundary to be estimated.

In paper of reference [19] was proposed to use graph cuts in a Bayesian framework for automatic initialization and propagate multiple mean parametric models derived from principal component analysis of shape and posterior probability information of the prostate region to segment the prostate. The authors of reference [20] presented a full automatic model based on a probabilistic framework for propagation of a parametric model derived from Principal Component Analysis (PCA) of prior shape and posterior probability values to achieve the prostate segmentation. In [21] is a method is proposed consists 4 main stages for prostate segmentation. For noise removing it uses a M3-Filter to generate a despeckled image. Then it is enhanced using morphological operations. In the third stage, The DBSCAN algorithm is applied to identify the core pixels, border pixels and noise pixels. The Clusters are formed by considering the density relations of the points. The clusters of core pixels and border pixels are used to automatically characterize the prostate region.

Mahdavi et a1. presented a 3D semi-automatic prostate segmentation method for B-mode trans-rectal ultrasound (TRUS) images [22]. Segmentation is based on prior knowledge of the prostate transversal section shape which is assumed to be a tapered ellipse. The approach consists of an initial untapering and warping of the image to make the shape of the prostate approximately elliptical. The prostate contour is found in the untapered, warped images by edge detection and 2D/3D ellipsoidal curve fitting, performed by solving convex optimization problem.

The authors of reference [23] proposed to use Haar wavelet approximation coefficients to extract texture features of the prostate region in both modalities to guide a deformable parametric model to segment the prostate in a multi-resolution framework. Principal Component Analysis (PCA) of the shape and texture information of the prostate region obtained from the training data aids contour propagation of the deformable parametric model. Prior knowledge of the optimization space is utilized for optimal segmentation of the prostate. In [24] was presented to use Haar wavelet approximation coefficients to extract texture features of the prostate region in both modalities to guide a deformable parametric model to segment the prostate in a multi-resolution framework. Principal Component Analysis (PCA) of the shape and texture information of the prostate region obtained from the training data aids contour propagation of the deformable parametric model. Prior knowledge of the optimization space is utilized for optimal segmentation of the prostate.

This paper consists 5 main sections. In section 2 the presented algorithm is introduced generally. section 3 to 5 present a detailed description for preprocessing, inside point detecting and segmentation steps respectively. Finally the achieved results of experiment, is presented in section 6.

2. PROSTATE SEGMENTATIOM SYSTEM

The segmentation system consists 3 stages, shown in Fig. 1. The first stage is the preprocessing step that includes sticks filter and the morphological smoothing. The sticks filter is used to eliminate speckle noise as it preserves the edges information. The morphological operations are top-hat and bottom-hat transform and it used for more smoothing. The second stage is the inside point detection that finds a pixel in prostate region. This pixel is a vital start point for segmentation. This stage includes 3 sub steps that are the threshold determining using a neural network system, the thresholding and the labeling and the region investigation. Finally prostate boundary is detected in the segmentation stage using GVF active contour algorithm.

3. PREPROCESSING

The preprocessing stage contains two subdivision that are noise removing and morphological smoothing. The noise in the input image is removed by applying sticks filter in the noise removing step [25]-[27]. After the noise removing step, roughness of image is reduced

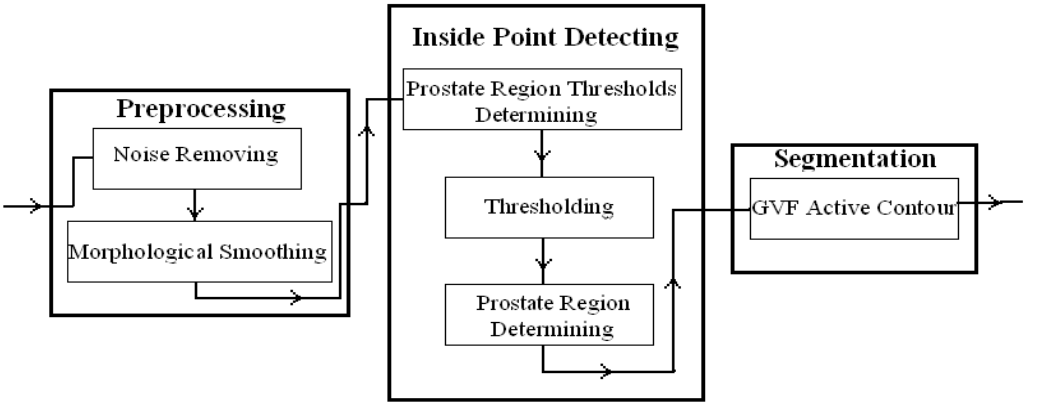

Fig. 1. System's algorithm

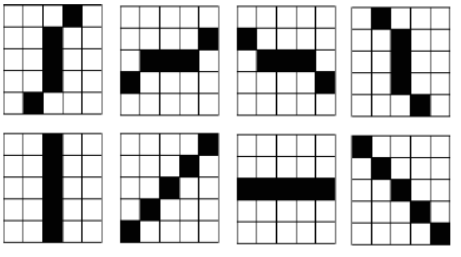

Fig. 2. Several windows for a sticks filter which length equals to 5. The White places are 0 and black places are 1/5

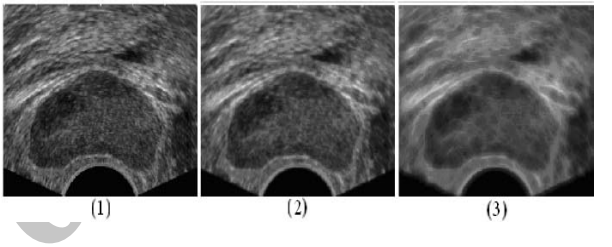

Fig. 3. (1) Input image, (2) filtered image by sticks filter with L=5, T=3, (3) filtered image by with L=15, T=1

by applying the morphological smoothing.

3.1. Noise Removing Using Sticks Filter

Further study of the performing low-pass filters and adaptive low-pass filters show that these filters, successfully eliminate most of the speckle noise but they cause a loss of details in low-contrast border regions. The stick's filter eliminates the speckle noise in ultrasound images without losing edge details. The Sticks filter is similar to spatial filtering but There is a main difference between this kind of filter and other spatial filters. Against usual filters which use a window for filtering the noise (such as averaging filter which has a window with length equal L and pixels equal 1/L), this kind of filter uses more than one window. The maximum number of possible orientation that the stick can be arranged in, determines the number of windows .On the other word for sticks filter with length equal L, there are 2L-2 orientation for sticks in a window. So, there are 2L-2 windows for a sticks filter with the length equal to L. A sample of windows for a sticks filter with the length equal to 5 are showed in Fig. 2. Equation (1) shows Mathematically the set of windows:

$$S = \left\{ s_{\theta_i} \mid_{L=1...2L-2} \right\} \quad (1)$$

That:

$$s_{\theta_i} = \begin{cases} \frac{1}{L} & if\ pixel\ along\ to\ \theta_i \\ 0 & otherwise \end{cases} \quad (2)$$

That S is set of windows, i is orientation, s_{θ_i} is window in the orientation of i and L is length of window. Then all of windows are convoluted in the main image. So 2L-2 the image will be obtained. The obtained set of images is showed as below:

$$H=\{h_i \mid i=1... \ 2L-2\} \quad (3)$$

Where

$$h_i = f * s_{\theta i} \quad (4)$$

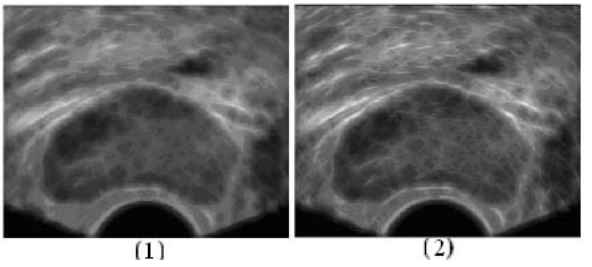

Fig. 4. (1) Output image of noise removing step, (2) output image of morphological smoothing

Filtered image got from the H, after a pixel by pixel investigation, such that:

$$g(x,y)=\max\{h_i(x,y)\}, \text{ for } i\ldots 2L-2. \quad (5)$$

Which in (3), (4) and (5) f is original image, g is the filtered image and H is the set of images which are obtained by convoluting original image with windows. Here the Stick's filter is used twice, for the noise removing and smoothing. A sticks filter with length equal to 5 and thickness equal to 3, in first step is used and a stick's filter with length equal to 15 and thickness equal to 1 is used in the second step. The Results of applying the stick's filter for a typical prostate TRUS image is shown in Fig. 3.

3.2. Morphological Smoothing:

The filtered image (F_a) obtained from the noise removing step has some roughness. The morphological smoothing step is used to remove roughness and enhance the contrast of around edges. Top-hat and bottom-hat transforms [28], [29] are used in morphological smoothing step and are applied to output image of the noise removing step. Here for top-hat and bottom-hat functions has used a disk with radius equal to 3. The smoothed image has been gotten from equation (6):

$$F_s = F_a + F_t - F_b \quad (6)$$

That:

$$F_t = top-hat(F_a) \quad (7)$$

$$F_b = bottom-hat(F_a) \quad (8)$$

F_t and F_b are the results of top-hat and bottom-hat transformations and F_s is the smoothed image. Results of applying the morphological smoothing step on the image obtained from the noise removing step is shown in Fig. 4.

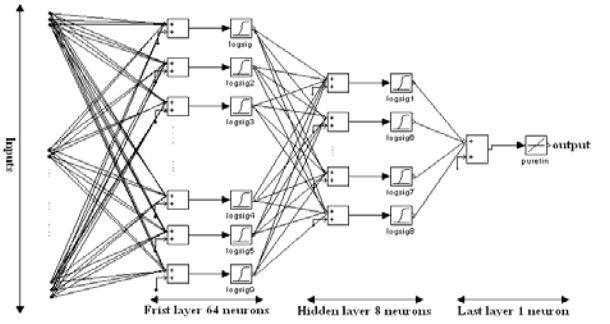

Fig. 5. 3 layers neural network

4. INSIDE POINT DETECTION:

The inside point detection contains three sub steps that are the prostate region thresholds determining, thresholding and finally, the prostate region determining. In the next sections, all of the steps are described in details.

4.1. Prostate Region Thresholds Determining:

Generally there is high roughness in TURS images and the objects are in this kind of images. So the preprocessing step is usually used to decrease this roughness. Although the preprocessing step decreases the roughness but it isn't good enough to obtain some critical thresholds using usual thresholding methods. Here, two feed forward neural network are employed to determine the prostate region thresholds. One of the networks is used to find the minimum threshold and other for the maximum threshold. These neural network have three layers which first layer has 64 neurons, second layer has 8 neurons and last layer has one neuron. The mentioned three layers- neural networks are shown in Fig. 5. The neural networks are trained by the back propagation method and their educational patterns are the average of pixels value in 200 central columns of smoothed image in preprocessing stage. The targets of the neural networks are the approximate thresholds (maximum threshold and minimum threshold) of the prostate region which is determined manually.

4.2. Thresholding:

Thresholding that is usually one of the main steps in the presented segmentation algorithms is applied in this step. The neural network outputs are used to convert the smoothed image to binary image. So the object with the biggest surface will be prostate region in the binary image after the thresholding.

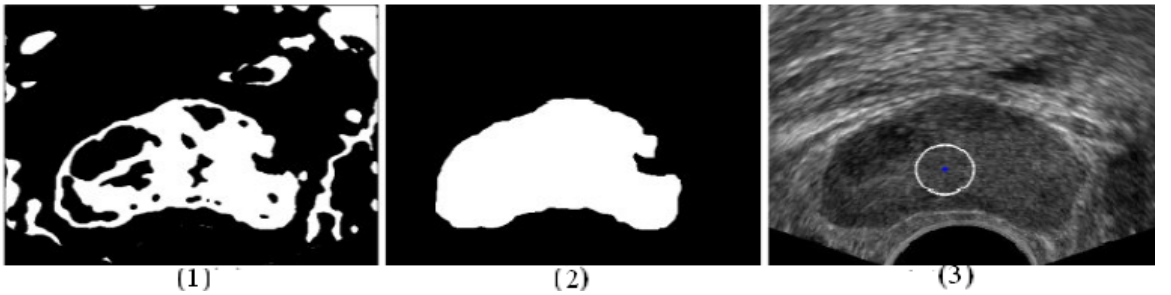

Fig. 6. (1) The binary image with using thresholds obtained by neural network, (2) object with biggest surface, (3) inside point inner prostate region

4.3. Prostate Region Determining:

The main target in this step is to obtain a point in the prostate region which was achieved by morphological operations. First, an erosion operand is applied on the binary image, which was gotten from the threshold step, to separate the extra region from the prostate region. A disk with the radius equal to 5 is used in erosion operand. Then the holes which are in the image are filled. Finally, an object that has the largest surface is known approximately as the prostate region and the point which is in its center will be an inner point of the prostate region, certainly. The obtained inner point is used to the prostate boundaries detection in the next step that is described and detailed in the next section. The results of applying the inside point detecting step on the image obtained from the noise removing step is shown in Fig. 6.

5. SEGMENTATION:

At first in this step, a contour is drawn around the inner point obtained before step by using graphic methods and then the contour using the active contour algorithm is expanded, until it reaches to the prostate boundary. Finally**,** the prostate boundaries are segmented in the image.

5.1. Active Contour Algorithm:

Active contour algorithm changes the contour form the searching to the suitable features within an object which is in the image [30]. The active contour can be defined as a n-points set of the points which are on the image that is known "controlled points" and it can be shown in equations (9) and (10):

$$V = \{v_1, v_2, v_3 \ .... \ v_n\} \tag{9}$$

$$v_i = (x_i, y_i) \tag{10}$$

That, (x_i, y_i) is coordination of V_i in the image. The points which are on the contour is moved to the object boundary in a repeatedly method as an equation which is called energy equation is minimized. The total equation of an active contour's energy function is as bellow (11):

$$E = \int \left[\frac{1}{2} \left(\alpha \left| v_i^{'} \right|^2 + \beta \left| v_i^{''} \right|^2 \right) + E_{ext}(v_i) \right] d(v_i) \tag{11}$$

That α, β are fixed coefficients that adjust bending and elastic energies. For minimizing the equation (11), active contour must satisfy the equation (12) which is called Oiler equation [15]:

$$\alpha v_i^{''} - \beta v_i^{''''} - \nabla E_{ext} = 0 \tag{12}$$

That ∇ is gradient operand. The proof of the equation (12) is presented in [25]. We can show the equation (11) as equation (13):

$$E_{contour} = E_{\text{int}} + E_{ext} = E_{bending} + E_{elastic} + E_{ext} \tag{13}$$

That $E_{elastic}$, $E_{bending}$ are elastic energy and bending energy respectively. Elastic energy determines expansion and contraction of the contour, and, it's form in the discrete domain is similar to (14):

$$E_{elastic} = \left\| v_{i+1} - v_i \right\| \tag{14}$$

The bending energy causes that the controlled points could permeate better in the corners and the bending regions. This energy is got from equation (15) in the discrete domain:

$$E_{bending} = \left\| v_{i+1} - 2v_i + v_{i-1} \right\| \tag{15}$$

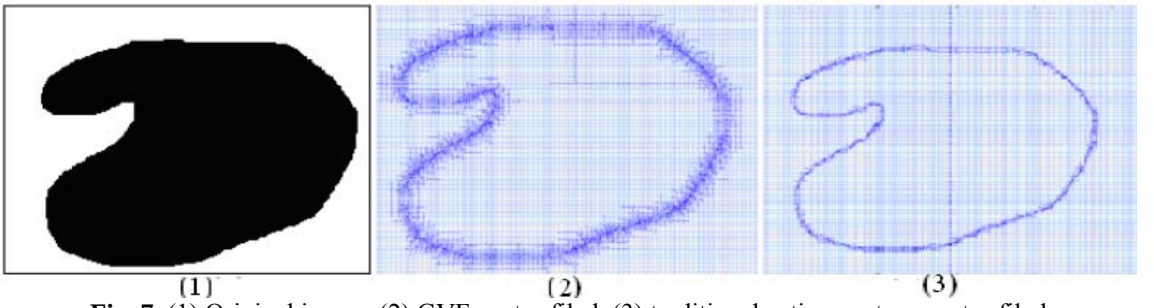

Fig. 7. (1) Original image, (2) GVF vector filed, (3) traditional active contour vector filed

5.2. GVF Active Contour:

The main difficulty of the traditional active contour is its external energy. The traditional active contour's external energy has low capture range. So, the active contour couldn't move the controlled points to the curve of objects. The low edges of the objects in the ultrasound images cause the traditional active contour's difficulties which are more obvious. For using active contour in the ultrasound images, we need an active contour which has an external energy with stronger capture range. The GVF active contour [31] has stronger capture range than traditional active contour (The active contour which has been presented in 5.1) so it's suitable for object segmentation in the ultrasound images. The external vector field of traditional active contour and GVF for a typical object are shown in Fig.7. it's visible that the field of GVF is stronger than traditional active contour's field. The GVF vector field is used instead of the external force in the equation (12). The field of GVF is defined so that it minimizes the energy function:

$$G(x,y)=[u(x,y),v(x,y)]$$
$$E=\iint\left[\mu(u_x^2+u_y^2+v_x^2+v_y^2)+|\nabla f|^2|G-\nabla f|^2\right]dxdy \quad (16)$$

That ∇f is the edge map which is defined:

$$f(x,y)=-E_{ext}(x,y) \quad (17)$$

The field of GVF is obtained through solving the Oiler's equation:

$$\mu\nabla^2 u-(u-f_x)(f_x^2+f_y^2)=0 \quad (18)$$

$$\mu\nabla^2 v-(v-f_y)(f_x^2+f_y^2)=0 \quad (19)$$

We can get a repeated algorithm for applying the active contour of GVF using (18) and (19).

6. RESULTS

In this paper a full automatic algorithm for prostate segmentation is presented in the TRUS images. The algorithm for noise removing used the stick's filter twice. First a stick's filter with length equal to 5 and thickness equal to 3 and then a stick's filter with length equal to 15 and thickness equal to 1 are used respectively . In the morphological smoothing step, the structuring element that was used in this step, is a disk with radios equal to 3 pixels. A 3 layers neural network is used to find an inner prostate region. Our data set includes 23 TRUS images whose 8 images were used to train the neural network. The neural networks were trained using the back propagation algorithm and their weights converged after 300 thousand epochs. Table 1 shows the value of extracted features for 15 selected test images that are obtained by using the trained neural networks manually. But the results applying of the presented algorithm on 15 TRUS images comprised with the results which had been abstained by the radiologist. For the comparison is used "Area Mean Square Error " that is defined as below:

$$AMSE=\frac{A_{man}-A_{algorithm}}{A_{man}}\times 100 \quad (20)$$

That A_{man} and $A_{algorithm}$ are the area of region that are segmented by the radiologist manually and the presented algorithm respectively. The obtained errors for 10 images are shown in Table 2 and Table 3 shows the statistical information of Table2.

The obtained results are demonstrated in table 2 by the kass active contour [30]. It is visible that the presented algorithm using the GVF active contour is achieved by the best results .The results of Table 2 show that the presented algorithm has better capability than the one proposed in [7]. The obtained output results of the proposed system for some images and the radiologist's opinion about it are shown in Fig 8.

Table1. The targets and it's neural network outputs for 15 typical TRUS images

Test images	Calculated Features Using Trained Neural Networks		Calculated Features Manually	
	Tlow	*Thigh*	*Tlow*	*Thigh*
1	0.122	0.285	0.117	0.292
2	0.175	0.383	0.176	0.386
3	0.128	0.293	0.101	0.269
4	0.163	0.375	0.170	0.312
5	0.227	0.343	0.209	0.362
6	0.175	0.341	0.179	0.357
7	0.179	0.439	0.138	0.418
8	0.207	0.409	0.209	0.404
9	0.187	0.426	0.137	0.398
10	0.119	0.294	0.108	0.284
11	0.121	0.301	0.115	0.336
12	0.149	0.476	0.183	0.433
13	0.279	0.457	0.234	0.448
14	0.257	0.408	0.241	0.433
15	0.326	0.446	0.342	0.492

Table 2. Area Mean Square Error between prostate region segmented by presented image and prostate region segmented by radiologist

Test images	AMSE Using Presented Algorithm	AMSE Using Kass Active Contour
1	3.18%	3.79%
2	4.4%	5.32%
3	2.22%	3.41%
4	0.047%	1.18%
5	2.84%	3.74%
6	0.037%	1.21%
7	1.35%	2.92%
8	0.87%	1.59%
9	0.034%	1.28%
10	1.54%	2.01%
11	0.25%	1.61%
12	3.54%	5.87%
13	1.49%	2.59%
14	0.58%	1.69%
15	0.44%	1.85%
Average	1.52%	2.67%

Table 3. Static information of table 2

Min	Max	Mean	Std
0.037%	4.4%	1.65%	1.54%

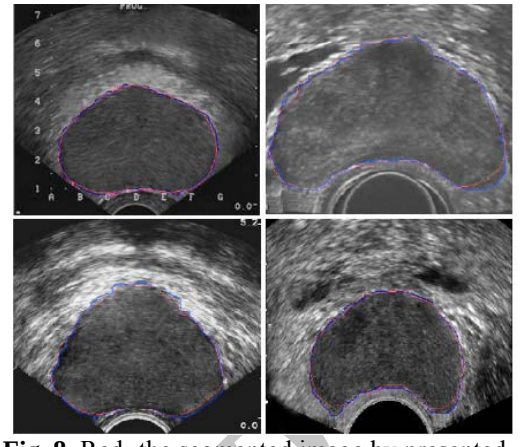

Fig. 8. Red- the segmented image by presented algorithm, blue-the manual segmented image by radiologist

7. CONCLUSION

In this study, we have presented a new algorithm for prostate segmentation in TRUS images. This algorithm also reduces speckle noise and it enhances the edge contrast. The presented algorithm consists 3 main stages. First step was the noise reduction by applying the stick filter and smoothing by the morphological operation.

In the second step for inside point finding, a three layers networks is used to find an inner prostate region point. In each sub network, 3 layers are used. The input layer has 64 neurons, the hidden layers are 8 neurons layers and the output layer is a 1 neuron layer. With using inside point prostate region and active contour algorithm, prostate boundaries are detected in the last stage.

Output Results show that the system which is presented in this article is a suitable system for automatic segmentation of prostate.

8. ACKNOWLEDGMENT

The authors wish to thank several people. we would like to thank Islamic azad University collection because this work has performed with their Financial Aids. We would also like to thank Dr. Bagheri and Dr. Shakiba, the two radiologists from shiraz namazi hospital for their helps and the images that they gave us.

REFERENCES

[1] Cancer Facts and Figures. American Cance Society. [Online] http://www.cancer.org, 2002.

[2] C., Mettlin, **"American society national cancer Detection project,"** Vol. 75, pp. 1790-1794, Cancer 1995.

[3] D., Sayan, Pathak, V., Chalana, D. R. Haynor, and K., Yongmin, **"Edge-guided boundary delineation prostate ultrasound images,"** I*EEE Trans. Med. Imaging*, Vol. 19, No. 12, pp. 1211-1219, 2000.

[4] M., Fitzpatrick and J. M., Reinhardt, editors, **"Prostate ultrasound image segmentation using**

level set-based region flow with shapeguidance," SPIE, Apr. 2005.

[5] A., Jendoubi, J., Zeng, and M. F., Chouikha, **"Top-down approach to segmentation of prostate boundaries in ultrasound images,"** In *AIPR*, pp. 145-149, 2004.

[6] F., Sahba, H. R., Tizhoosh, and M. A., Magdy Salama, **"Segmentation of prostate boundaries using regional contrast enhancement,"** In the *IEEE International Conference on Image Processing (ICIP)*, Vol. 2, pp. 1266-1269, Sept. 2005.

[7] F., Sahba, H. R., Tizhoosh, and M. A., Magdy Salama, **"A coarse-to-fine approach to prostate boundary segmentation in ultrasound images,"** *Bio Medical Engineering OnLine*, 2005.

[8] C. K., Kwoh, M., Teo, W., Ng, S,. Tan, and M., Jones, **"Outlining the prostate boundary using the harmonics method,"** *Med. Biol. Eng. Computing*, Vol. 36, pp. 768–771, 1998.

[9] .G., Aarnink, R. J. B., Giesen, A. L., Huynen, J. J. de la Rosette, F. M., Debruyne, and H., Wijkstra, **"A practical clinical method for contour determination in ultrasound prostate images,"** *Ultrasound Med. Biol.*, Vol. 20, pp. 705–717, 1994.

[10] R. G., Aarnink, S. D., Pathak, J. J. de la Rosette, F. M., Debruyne, Y., Kim and H., Wijkstra, **"Edge detection in ultrasound prostate images using integrated edge map,"** *Ultrasound Med. Biol.*, Vol. 36, pp. 635–642, 1998.

[11] Y., Zhan and D., Shen, **"Deformable segmentation of 3-d ultrasound prostate images using statistical texture matching method,"** *IEEE Transactions on Medical Imaging*, Vol. 25, pp. 256–272, 2006.

[12] D., Freedman, R. J., Radke, T., Zhang, Y., Jeong, D. M., Lovelock, and G. T. Y., Chen, **"Modelbased segmentation of medical imagery by matching distributions,"** *IEEE Transactions on Medical Imaging*, Vol. 24, pp. 281–292, 2005.

[13] A., Ghanei, H., Soltanian-Zadeh, A., Ratkewicz, and F., Yin, **"A three dimentional deformable model for segmentation of human prostate from ultrasound images,"** *Med. Phys*, Vol. 28, pp. 2147–2153, 2001.

[14] C., Knoll, M., Alcaniz, V., Grau, C., Monserrat, and M,. Juan, **"Outlining of the prostate using snakes with restrictions based on the wavelet transform,"** *Pattern Recognition*, Vol. 32, pp. 1767–1781, 1999.

[15] S. D., Pathak, V., Chalana, D., haynor, and Y., kim, **"Edge guided boundary delineationin prostate ultrasound images,"** *IEEE Transactions on Medical Imaging*, Vol. 19, pp. 1211–1219, 2000.

[16] N. N., Kachouie, P., Fieguth, **"A Medical Texture Local Binary Pattern For TRUS Prostate Segmentation,"** 29th *Annual International conference of Engineering in Medicine and Biology Society*. pp 5605-5608, 2007.

[17] P., Yan, S., Xu, B., Turkbey , J., Kruecker, **"Discrete Deformable Model Guided by Partial Active Shape Model for TRUS Image Segmentation,"** *IEEE Transaction on Biomedical Engineering*, Vol. 57, No. 5, May 2010.

[18] S. S., Mohamad, M. MA., Salama **"Spectral clustering for TRUS images,"** *BioMedical Engineering OnLine*, 2007.

[19] S., Ghose, A., Oliver, R., Martin, X., Liado, J., Freixente, J., Martin, **"Statistical Shape and Probability Prior Model for Automatic Prostate Segmentation,"** *International Conference on Digital Image Computing Techniques and Applications (DICTA)*, pp. 340-345, 2011.

[20] S., Ghose, A., Oliver, R., Martin, X., Liado, J., Freixente, J., Martin, **"A probabilistic framework for automatic prostate segmentation with a statistical model of shape and appearance,"** Image Processing (ICIP), 2011 18th *IEEE International Conference*, pp. 713-716, 2011.

[21] R., Manavalan, K., Thangavel, **"TRUS image segmentation using morphological operators and DBSCAN clustering,"** *Information and Communication Technologies (WICT)*, World Congress, pp. 898-903, 2011.

[22] S., Mahdaviani, E., Septimiu **"3D prostate segmentation based on ellipsoid fitting, image tapering and warping,"** *Engineering in Medicine and Biology Society, EMBS. 30th Annual International Conference of the IEEE*, pp. 2988-2991, 2008.

[23] S., Ghose, A., Oliver, R., Martin, X., Liado, J., Freixente **"Prostate Segmentation with Texture Enhanced Active Appearance Model,"** *Signal-Image Technology and Internet-Based Systems (SITIS), Sixth International Conference*, pp. 18-22, 2010.

[24] S., Ghose, A., Oliver, R., Martin, X., Liado, J., Freixente, **"Spectral clustering of shape and probability prior models for automatic prostate segmentation,"** *Engineering in Medicine and Biology Society (EMBC) Annual International Conference of the IEEE*, pp. 2335-2338, 2012.

[25] Y. Wang, H. N., Cardinal, D. B., Downey, A., Fenster, **"Semiautomatic three-dimensional segmentation of the prostate using two dimensional ultrasound images,"** *Medical physics*, Vol. 30, No. 5, pp. 887-897, 2003.

[26] R. N., Czerwinski, D. L., Jones, and W. D., O'Brien Jr., **"Detection of lines and boundaries in speckle images,"** application to medical ultrasound, *IEEE Trans. on Medical Imaging*, Vol. 18, No. 2, pp. 126-136, Feb. 1999.

[27] R. N., Czerwinski, D. L., Jones, and W. D., O'Brien Jr., **"Line and boundary detection in speckle images,"** .*IEEE Trans. on Image Processing*, Vol. 7, No. 12, pp. 1700-1714, Dec. 1998.

[28] R. C., Gonzalez, and R. E., Woods, **"Digital Image Processing,"** 2nd. Ed. Prentice-Hall, 2002.

[29] R. C., Gonzalez, and R. E., Woods, **"Digital Image Processing using matlab,"** Ed. Prentice-Hall, 2004.

[30] M., Kass, A., Witkin, and D., Terzopoulos, **"Snakes: Active contour models,"** *International Journal of Computer Vision*, pp. 321-331, 1988.

[31] Ch., Sun, and K. M., Lam, **"The GVF Snake with a Minimal Path Approach,"** 6th *IEEE/ACIS International Conference on Computer and Information Science*, 2007.